

# Neuron–Astrocyte Interactions, Pyruvate Carboxylation and the Pentose Phosphate Pathway in the Neonatal Rat Brain

Tora Sund Morken <sup>1</sup>

Eva Brekke <sup>2</sup>

Asta Håberg <sup>2</sup>

Marius Widerøe <sup>3</sup>

Ann-Mari Brubakk <sup>1,4</sup>

Ursula Sonnewald <sup>2,\*</sup>

Phone: +47-73-590492

Fax: +47-55-1350

Email: ursula.sonnewald@ntnu.no

<sup>1</sup> Department of Laboratory Medicine, Children's and Women's Health, Norwegian University of Science and Technology (NTNU), 7489, Trondheim, Norway.

<sup>2</sup> Department of Neuroscience, INM, Medical Faculty, Norwegian University of Science and Technology (NTNU), MTF5, 7489, Trondheim, Norway.

<sup>3</sup> Department of Circulation and Medical Imaging, Norwegian University of Science and Technology, 7489, Trondheim, Norway.

<sup>4</sup> Department of Pediatrics, St. Olav University Hospital, Central Norway Regional Health Authority, 7006, Trondheim, Norway.

---

## Abstract

Glucose and acetate metabolism and the synthesis of amino acid neurotransmitters, anaplerosis, glutamate-glutamine cycling and the pentose phosphate pathway (PPP) have been extensively investigated in the adult, but not the neonatal rat brain. To do this, 7 day postnatal (P7) rats were injected with [1-<sup>13</sup>C]glucose and [1,2-<sup>13</sup>C]acetate and sacrificed 5, 10, 15, 30 and 45 min later. Adult rats were injected and sacrificed after 15 min. To analyse pyruvate carboxylation and PPP activity during development, P7 rats received [1,2-<sup>13</sup>C]glucose and were sacrificed 30 min later. Brain extracts were analysed using <sup>1</sup>H- and <sup>13</sup>C-NMR spectroscopy. The neonatal brain contained lower levels of glutamate, aspartate and *N*-acetylaspartate but similar levels of GABA and glutamine compared to adults. Metabolism of [1-<sup>13</sup>C]glucose at the acetyl CoA stage was reduced much more than that of [1,2-<sup>13</sup>C]acetate. The transfer of glutamate from neurons to astrocytes was greatly reduced while transfer of glutamine from astrocytes to glutamatergic neurons was relatively higher compared to adults. However, transport of glutamine from astrocytes to GABAergic neurons was lower. Using [1,2-<sup>13</sup>C]glucose it could be shown that despite much lower pyruvate carboxylation, relatively more pyruvate from glycolysis was directed towards anaplerosis than pyruvate dehydrogenation in astrocytes compared to reports from the adult brain. Moreover, the ratio of PPP/glucose metabolism was higher in P7 compared to adult brain. Our findings indicate that only the part of the glutamate-glutamine cycle that transfers glutamine from astrocytes to neurons is operating in the

neonatal brain and that compared to adults, relatively more glucose is prioritised to PPP and pyruvate carboxylation. These findings may have implications for the capacity to protect the neonatal brain against excitotoxicity and oxidative stress.

---

## Keywords

Neonatal

Brain

Glutamate-glutamine cycle

Pyruvate carboxylation

Pentose-phosphate-pathway

$^{13}\text{C}$ -NMR spectroscopy

## Introduction

Glucose is the main substrate for the adult brain. Its metabolites are used for energy production, tricarboxylic acid (TCA) cycle function and neurotransmitter synthesis whereas in the neonatal brain alternate substrates like ketone bodies are used [1, 2]. In order to be metabolised, these substrates must pass the blood–brain-barrier (BBB). Ketone bodies have high rates of transport via specific monocarboxylate transporters (MCTs) until weaning, when the expression of MCT1, the major transporter in the BBB, decreases quickly, while that of glucose transporters increases [3]. Acetate is transported via the same transporters as ketone bodies and is thus an excellent tool to probe ketone body transport [4]. In the adult brain acetate is exclusively metabolised in astrocytes [5] whereas it has been calculated that at the acetyl CoA level approximately 70 % of the available glucose in the adult brain is metabolised by neurons [6]. In the neonatal brain it is conceivable that acetate is utilised by both neurons and astrocytes since MCTs are observed on both [3]. Nuclear magnetic resonance spectroscopy (NMRS) with [1,2- $^{13}\text{C}$ ]acetate can be used to probe this.

After uptake into the cell, glucose (via pyruvate from glycolysis) and acetate can be converted to the TCA cycle substrate acetyl CoA. It has been reported that glucose oxidation is lower and that the average time the metabolites stay in the TCA cycle before conversion to substances such as neurotransmitters glutamate and thereafter  $\gamma$ -amino butyric acid (GABA) is longer in the neonatal compared to the adult brain [7]. This is in part attributed to the low levels of enzymes for pyruvate metabolism and oxidative glucose metabolism in the postnatal period [8].

Pyruvate carboxylase, the brain's exclusive anaplerotic enzyme [9], is present in astrocytes only [10], and is of major importance for glial metabolic support of neurotransmission. Pyruvate carboxylase content is low in the neonatal period and increases 15-fold up to young adult age (postnatal day 30–40) when the level reaches a plateau [8].

Most of the glutamate in the brain is found in neurons and is released into the synapse after depolarisation [11]. The ability of astrocytes to take up glutamate from the synapse and convert it into glutamine by the astrocyte specific enzyme glutamine synthetase [12] is vital for normal metabolic homeostasis and as a defence mechanism against excitotoxicity [13]. The subsequent transfer of glutamine from astrocytes to neurons for deamidation to glutamate closes the glutamate-

glutamine cycle. The number of glutamine transporters on astrocytes (SN1) on postnatal day seven (P7) is similar to adult levels but increases over the next 7 days and peaks on P14 with twice the number found on adult astrocytes, paralleling the synaptogenetic spurt period [14, 15]. Neuronal glutamine transporters are also present on postnatal day 7 [16], setting the stage for transport of glutamine from astrocytes to neurons and the subsequent utilisation of glutamine for glutamate synthesis. Expression of the predominantly astrocytic glutamate transporters GLT-1 on astrocytes is low in the neonatal brain [17] possibly limiting the ability of astrocytes to rapidly reduce the glutamate concentration in the synaptic cleft, and thus increasing the danger of excitotoxic events. However, the actual cycling of glutamate and glutamine between the neuronal and astrocytic compartments has not been characterised in the neonatal brain.

$\gamma$ -Amino butyric acid is known to be excitatory in the neonatal brain and its level has been reported to be similar to the adult brain [18]. Thus, GABA release may be crucial for signalling between nerve cells during early brain development. However, the homeostasis of GABA in the neonatal brain has not been explored in detail.

Although alternative substrates for energy production are of major importance in the developing brain, the presence of glucose is essential [1]. This is in part due to the fact that the pentose phosphate pathway (PPP) requires glucose-6-P. In early brain development there is a need for production of nucleotides for DNA synthesis. Furthermore, myelination begins during the first postnatal week in the rat with a concurrent need for NADPH for lipid synthesis and the regeneration of reduced glutathione (GSH) [19, 20]. These needs can be met by the PPP, which produces nucleotides and NADPH. Earlier studies have shown that the pathway accounts for approximately 2–5 % [21–23] of the glucose metabolism in the adult brain and can be upregulated to 9–20 % in response to injury in animal and human studies [24, 25]. However, little is known about the PPP in the developing brain.

The aim of the present study was to characterise metabolic pathways for glucose and acetate and neuronal-astrocytic interactions in the neonatal brain, and compare these to those in the adults. [1,2-<sup>13</sup>C]glucose and [1-<sup>13</sup>C]glucose probe predominately neuronal metabolism whereas [1,2-<sup>13</sup>C]acetate probes primarily astrocytic metabolism [5]. Our aims were to analyse: (1) if the utilisation, cycling and incorporation of [<sup>13</sup>C]glucose would be lower; (2) if the relative proportion of [<sup>13</sup>C]glucose metabolised via the pentose phosphate and pyruvate carboxylation pathways would be larger; (3) the different transfers of substrate between the cellular compartments in the neonatal versus the adult brain.

## Materials and Methods

### Materials

Sprague–Dawley rats were purchased from Scanbur AS, Norway. The average bodyweight of the P7 pups was  $12.6 \pm 0.1$  g and for adult rats  $250 \pm 10$  g. [1-<sup>13</sup>C]glucose, [1,2-<sup>13</sup>C]glucose and [1,2-<sup>13</sup>C]acetate (99 % <sup>13</sup>C enriched) were from Cambridge Isotope Laboratories (Woburn, MA, USA), D<sub>2</sub>O (99,9 %) from CDN Isotopes (Pointe-Claire, Canada), ethylene glycol from Acros Organics (Geel, Belgium) and 3-(trimethylsilyl)-1-propane-sulfonic acid (DDS) from Sigma-Aldrich (St. Louis, MA, USA). All other chemicals were of the purest grade available from regular commercial sources.

## Methods

### *Animal Procedures*

All experiments were approved by the Animal Care and Use Committee at the Norwegian University of Science and Technology (Forsøksdyrutvalget). Postnatal day seven (P7) Sprague–Dawley rats of both genders were injected intraperitoneally (ip.) with [1-<sup>13</sup>C]glucose (543 mg/kg, 0.3 M) and [1,2-<sup>13</sup>C]acetate (504 mg/kg, 0.6 M) and decapitated 5, 10, 15, 30 and 45 min after injection (n = 3–4 at each time-point). One group of P7 rats (n = 4) was injected with [1,2-<sup>13</sup>C]glucose (564 mg/kg, 0.3 M) and decapitated after 30 min. In separate experiments, male adult rats (~3 months old, n = 10) were injected ip. with [1-<sup>13</sup>C]glucose (543 mg/kg, 0.3 M) and [1,2-<sup>13</sup>C]acetate (504 mg/kg, 0.6 M) and decapitated after 15 min. Heads were snap-frozen in liquid N<sub>2</sub> and stored at –80 °C until extraction.

### *Extraction*

Entire cerebri (P7) and cortex cerebri (adults) were dissected and extracted using perchloric acid (PCA) or with methanol-chloroform extraction (P7: 30 and 45 min). 7 % PCA was added and tissue was homogenized using a Vibra Cell sonicator (Model VCX 750, Sonics & Materials, Newtown, CT, USA). The homogenates were centrifuged at 3,000×g at 4 °C for 5 min. The neutralised supernatants were lyophilized and re-suspended in D<sub>2</sub>O before being lyophilized once more in order to minimize the proton content of water. When methanol-chloroform extraction was applied, methanol was added and tissue was homogenized using the same sonicator. Subsequently, chloroform and water were added, the samples were centrifuged at 3,000×g for 15 min and the supernatants were transferred to a new tube. Water was added to the second tube and the samples were centrifuged at 3,000×g for 15 min in order to separate the lipids from the supernatant with intracellular extracts. Finally, the supernatant was lyophilized, and treated as described above.

### *<sup>13</sup>C NMR-Spectroscopy and <sup>1</sup>H NMR-Spectroscopy*

Lyophilized samples were dissolved in 400 µl D<sub>2</sub>O containing 0.01 % ethylene glycol and 18.2 % DDS. The supernatants were transferred to SampleJet tubes (5.0 × 103.5 mm) for insertion into the SampleJet autosampler (Bruker BioSpin GmbH, Rheinstetten, Germany). All samples were analysed using a QCI CryoProbe™ 600 MHz on a 14.1T Ultrashielded Plus Avance III magnet (Bruker BioSpin GmbH, Rheinstetten, Germany) operating at 600 MHz using a QCI CryoProbe™. Proton decoupled <sup>13</sup>C NMR spectra were obtained using an acquisition time of 1.7 s, a relaxation delay of 0.5 s and a flip angle of 30°. Scans were accumulated at 30 kHz spectral width with 98 K data points. The number of scans was typically 2,400. The same spectrometer was used to obtain the <sup>1</sup>H NMR spectra. Scans were accumulated with a pulse angle of 90°, acquisition time was 2.7 s and relaxation delay was 10 s. The number of scans was 32. Relevant peaks in the spectra were identified and integrated using TopSpin™ 3.0 software (Bruker BioSpin GmbH, Rheinstetten, Germany). Concentrations of metabolites were calculated from the integrals of the peaks using DSS (<sup>1</sup>H NMR spectra) or ethylene glycol (<sup>13</sup>C NMR spectra) as internal quantification standards.

### *Amounts of Metabolites, <sup>13</sup>C Label and % <sup>13</sup>C Enrichment*

Concentrations from the <sup>1</sup>H NMR spectra were corrected for the numbers of protons that constituted the peak and for <sup>13</sup>C containing metabolites. The integrals from the <sup>13</sup>C NMR spectra were corrected for nuclear Overhauser and relaxation effects, and singlets in the <sup>13</sup>C spectra were,

when appropriate, corrected for natural abundance of  $^{13}\text{C}$  (1.1 %) calculated from the  $^1\text{H}$  spectra. All amounts were corrected for tissue weight. %  $^{13}\text{C}$  excess enrichment was calculated from the amounts of label corrected for natural abundance over the total amount of metabolite and will in the following be called %  $^{13}\text{C}$  enrichment. It should be noted that due to the euthanasia method used in the present study some post mortem effects were unavoidable. It is well known that GABA content increases with time after death and comparing our results with the in vivo data from Tkac et al. [18] it is apparent that the value of GABA is indeed increased. However, since the euthanasia methods were the same for postnatal and adult rats, amounts should be comparable. When evaluating amounts of glutamate, glutamine and aspartate between our study and that of Tkac et al. [18] no differences were evident.

## Glucose % Enrichment

Glucose % enrichment was calculated from  $\alpha$ -glucose satellites in the  $^1\text{H}$  NMR spectra, representing protons on the  $^{13}\text{C}$  labelled glucose in the  $\alpha$ -C1 position over the sum of  $\alpha$ -glucose and its satellites.

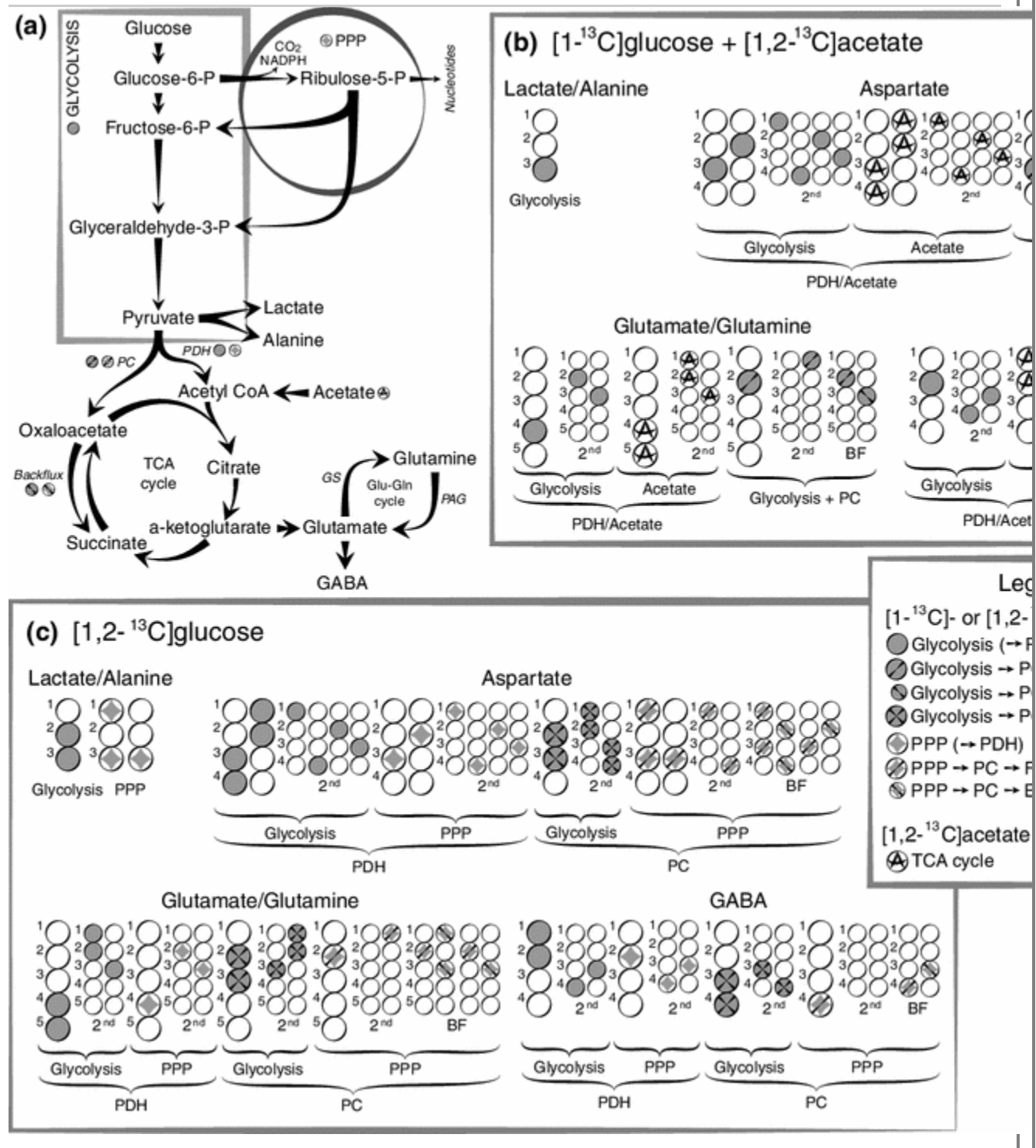
### Labelling Patterns After Injection of [1- $^{13}\text{C}$ ]Glucose (Fig. 1a, b)

Via glycolysis, [1- $^{13}\text{C}$ ]glucose will yield one unlabelled pyruvate (not considered further) and one [3- $^{13}\text{C}$ ]pyruvate molecule which can enter the TCA cycle as [2- $^{13}\text{C}$ ]acetyl CoA via PDH after condensation with oxaloacetate. After several steps  $\alpha$ -[4- $^{13}\text{C}$ ]ketoglutarate will be formed and can give rise to [4- $^{13}\text{C}$ ]glutamate, [4- $^{13}\text{C}$ ]glutamine and [2- $^{13}\text{C}$ ]GABA (from [4- $^{13}\text{C}$ ]glutamate). If  $\alpha$ -[4- $^{13}\text{C}$ ]ketoglutarate stays in the cycle, the  $^{13}\text{C}$  label will be scrambled in the symmetrical molecule succinate to yield equal parts of [2- $^{13}\text{C}$ ] or [3- $^{13}\text{C}$ ]succinate, fumarate, malate, oxaloacetate and aspartate. [2- $^{13}\text{C}$ ] or [3- $^{13}\text{C}$ ]oxaloacetate can condense with acetyl CoA and yield, [2- $^{13}\text{C}$ ] or [3- $^{13}\text{C}$ ]glutamate/glutamine and [3- $^{13}\text{C}$ ] or [4- $^{13}\text{C}$ ]GABA from the 2nd turn of the TCA cycle if the acetyl-CoA is unlabelled. If labelled, the molecules will in addition be labelled in the positions mentioned above from the 1st turn of the TCA cycle.

Fig. 1

Simplified presentation of  $^{13}\text{C}$  labeling patterns of metabolites following injection of [1- $^{13}\text{C}$ ]glucose and [1,2- $^{13}\text{C}$ ]acetate, or [1,2- $^{13}\text{C}$ ]glucose. **a** An overview over the principal metabolic pathways discussed. **b** The labeling patterns in lactate, alanine, aspartate, glutamate, glutamine and GABA following metabolism of [1- $^{13}\text{C}$ ]glucose and [1,2- $^{13}\text{C}$ ]acetate. **c** The labeling patterns in the same metabolites following metabolism of [1,2- $^{13}\text{C}$ ]glucose. The circles symbolise the carbon backbone of the molecules. *Dark grey filled circles mark* the position of the label resulting from glycolysis, followed by conversion to acetyl CoA by PDH where applicable. *A middle line crossing the dark grey circle* indicates that the pyruvate has instead undergone pyruvate carboxylation before being converted to the metabolite depicted. *The direction of the middle line* indicates if the pattern is derived from backflux or not. *Two lines crossing* indicate that the labeling pattern from backflux cannot be distinguished from the labeling pattern from forwardflux. An "a" in the *middle of the circle* indicates that the labeling pattern is derived from [1,2- $^{13}\text{C}$ ]acetate metabolism. *Light grey diamonds mark* the position of the label resulting from the PPP. The middle lines crossing symbolize the same as mentioned above. For simplicity, only condensation of oxaloacetate with unlabeled acetyl CoA is shown for the 2nd turn.  $\alpha$ -KG,  $\alpha$ -ketoglutarate; BF, backflux; gln, glutamine; glu, glutamate; GS, glutamine synthetase; P, phosphate; PAG, phosphate

activated glutaminase; PC, pyruvate carboxylase; PDH, pyruvate dehydrogenase; PPP, pentose phosphate pathway



**Labelling Patterns After Injection of [1,2-<sup>13</sup>C]Acetate (Fig. 1a, b)**

[1,2-<sup>13</sup>C]acetate will enter the TCA cycle via acetyl CoA and yield [4,5-<sup>13</sup>C]glutamate/glutamine and [1,2-<sup>13</sup>C]GABA. If the label remains in the TCA cycle for a 2nd turn, it will lead to glutamate and glutamine equally labelled in either [1,2-<sup>13</sup>C] or [3-<sup>13</sup>C]glutamate/glutamine and [3-<sup>13</sup>C] or [4-<sup>13</sup>C]GABA.

### **Labelling Patterns After Injection of [1,2-<sup>13</sup>C]Glucose (Fig. 1a, c)**

Using [1,2-<sup>13</sup>C]glucose it is possible to distinguish the labelling patterns in metabolites derived from the PPP from those resulting from glycolysis. In contrast to [1-<sup>13</sup>C]glucose from which the label will be lost as <sup>13</sup>CO<sub>2</sub>, [1,2-<sup>13</sup>C]glucose will retain the <sup>13</sup>C atom in the C2 position if metabolised via PPP. [1-<sup>13</sup>C]ribulose is formed from [1,2-<sup>13</sup>C]glucose. Three molecules of [1-<sup>13</sup>C]ribulose are involved when [1,3-<sup>13</sup>C]- and [1-<sup>13</sup>C]fructose-6-P as well as one unlabelled glyceraldehyde are formed. The labelled [1,3-<sup>13</sup>C]- and [1-<sup>13</sup>C]fructose-6-P will generate [1,3-<sup>13</sup>C]- and [3-<sup>13</sup>C]glyceraldehyde and subsequently pyruvate labelled in the same positions [26]. Three molecules of [1,2-<sup>13</sup>C]glucose will generate one [1,3-<sup>13</sup>C]pyruvate, one [3-<sup>13</sup>C]pyruvate and three unlabelled molecules of pyruvate which can either enter the TCA cycle and lead to labelling in glutamate/glutamine/GABA, or be reduced to lactate or transaminated to alanine maintaining the same labelling patterns as pyruvate. The sum of [1,3-<sup>13</sup>C]- and [3-<sup>13</sup>C]lactate/alanine can be quantified in the C3-positions in the spectra. Via PDH TCA cycle intermediates [4-<sup>13</sup>C]glutamate/glutamine and subsequently [2-<sup>13</sup>C]GABA can be formed from the 1st turn. PPP followed by PC will generate label in [2-<sup>13</sup>C]glutamate/glutamine and [4-<sup>13</sup>C]GABA. The part of the labelled oxaloacetate which backfluxes to the symmetrical molecule fumarate before it is again reverted to oxaloacetate, can be detected due to the formation of [3-<sup>13</sup>C]glutamate/glutamine and [3-<sup>13</sup>C]GABA which appears in addition to [2-<sup>13</sup>C]glutamate/glutamine and [4-<sup>13</sup>C]GABA. Via glycolysis, 3 molecules of [1,2-<sup>13</sup>C]glucose will generate three molecules of [2,3-<sup>13</sup>C]pyruvate and three unlabelled molecules of pyruvate, with corresponding labelling patterns in lactate and alanine. If this pyruvate is metabolised via PDH, the 1st turn of the TCA cycle will lead to formation of α-[4,5-<sup>13</sup>C]ketoglutarate and thus [4,5-<sup>13</sup>C]glutamate/glutamine and [1,2-<sup>13</sup>C]GABA. If [2,3-<sup>13</sup>C]pyruvate is carboxylated to [2,3-<sup>13</sup>C]oxaloacetate, this will yield [2,3-<sup>13</sup>C]glutamate/glutamine/aspartate and [3,4-<sup>13</sup>C]GABA.

### **Pyruvate Recycling**

A possible confounding factor to the interpretation of the labelling patterns described earlier would be the presence of extensive pyruvate recycling [27, 28]. After injection of [1,2-<sup>13</sup>C]glucose pyruvate recycling would lead to formation of [1-<sup>13</sup>C] or [2-<sup>13</sup>C] or [1,2-<sup>13</sup>C]acetyl CoA which could lead to singlet or doublet formation in the C4 and C5-positions of glutamate and glutamine. Since [4-<sup>13</sup>C]glutamate is also labelled from PPP derived metabolites, quantification of the amounts of [5-<sup>13</sup>C]glutamate and [5-<sup>13</sup>C]glutamine was used to evaluate this possibility.

## **Metabolic Ratios (See Sections Above and Fig. 1 for Explanation of Labelling Patterns)**

### **Acetate/Glucose Utilisation Ratio**

The acetate/glucose utilisation ratio in glutamate, GABA and glutamine gives the relative contribution of acetate and glucose to the labelling of these compounds which in the adult brain reflects mainly astrocytic (glutamine) and neuronal (glutamate and GABA) metabolism.

The following equations were used:

$$\left[4, 5\text{-}^{13}\text{C}\right] \text{glutamate}(\text{glutamine}) / \left[4\text{-}^{13}\text{C}\right] \text{glutamate}(\text{glutamine}) \quad (1)$$

$$\left[1, 2\text{-}^{13}\text{C}\right]\text{GABA} / \left[2\text{-}^{13}\text{C}\right]\text{GABA} \quad (2)$$

### Pentose Phosphate Pathway (PPP)/Glucose Metabolism Ratio (Fig. 1)

The sum of labelling via the PPP and glycolysis is called glucose metabolism (GM). Due to redistribution of the carbon atoms within the PPP, two labelled molecules of pyruvate correspond to the utilisation of three molecules of  $[1,2\text{-}^{13}\text{C}]$ glucose. While, when metabolised via glycolysis, three labelled molecules of pyruvate correspond to the utilisation of the same number of  $[1,2\text{-}^{13}\text{C}]$ glucose molecules. Thus, all values representing the PPP must be multiplied by 1.5 to adjust for this difference.

The PPP/GM ratio for lactate and alanine is therefore calculated as:

$$\left[3\text{-}^{13}\text{C}\right]\text{lactate(alanine)} \times 1.5 / \left( \left[2, 3\text{-}^{13}\text{C}\right]\text{lactate(alanine)} + \left[3\text{-}^{13}\text{C}\right]\text{lactate(alanine)} \times (1.5) \right)$$

If the pyruvate is further metabolised via PDH the PPP/GM ratio for glutamate and glutamine can be calculated as:

$$\left[3\text{-}^{13}\text{C}\right]\text{glutamate(glutamine)} \times 1.5 / \left( \left[4, 5\text{-}^{13}\text{C}\right]\text{glutamate(glutamine)} + \left[4\text{-}^{13}\text{C}\right]\text{glutamate(glutamine)} \times (1.5) \right)$$

It should be noted that this equation does not include labelling via PC, and may thus be less suited for calculation of the PPP/GM ratio in the astrocytic compartment.

### Pyruvate Carboxylase/Pyruvate Dehydrogenase (PC/PDH) Ratio

The ratio of flux via PC, which can only be found in astrocytes [10], versus flux via PDH, which is present in both neurons and astrocytes, was calculated for glutamate and glutamine from  $[1,2\text{-}^{13}\text{C}]$ glucose metabolism.

The PC/PDH ratio for glutamate and glutamine is calculated as:

$$\left[2, 3\text{-}^{13}\text{C}\right]\text{glutamate(glutamine)} / \left[4, 5\text{-}^{13}\text{C}\right]\text{glutamate(glutamine)} \quad (5)$$

For GABA the PC/PDH ratio will be:

$$\left[3, 4\text{-}^{13}\text{C}\right]\text{GABA} / \left[1, 2\text{-}^{13}\text{C}\right]\text{GABA} \quad (6)$$

### Pyruvate Carboxylase/Pyruvate Metabolism Ratio

The labelling patterns derived from  $[1,2\text{-}^{13}\text{C}]$ glucose can be combined from several metabolites to calculate a more over-all ratio for the contribution of PC to metabolism of glucose at the level of pyruvate (pyruvate metabolism). It was a ratio of the sum of 1st turn labelling from PC in



glutamate, glutamine, aspartate and GABA over the sum of 1st turn labelling from both PC and PDH activity in the same metabolites, giving rise to an approximation for the ratio for total PC/total pyruvate metabolism ( $PC_{tot}/PM_{tot}$ ):

$$\frac{\left[2, 3-^{13}\text{C}\right]\text{glutamate} + \left[2, 3-^{13}\text{C}\right]\text{glutamine} + \left[3, 4-^{13}\text{C}\right]\text{GABA} + \left[2, 3-^{13}\text{C}\right]\text{aspartate}}{\left(\left[4, 5-^{13}\text{C}\right]\text{glutamate} + \left[4, 5-^{13}\text{C}\right]\text{glutamine} + \left[1, 2-^{13}\text{C}\right]\text{GABA} + \left[1, 2-^{13}\text{C}\right]\text{aspartate} + \left[3, 4-^{13}\text{C}\right]\text{aspartate} + \left[2, 3-^{13}\text{C}\right]\text{glutamate} + \left[2, 3-^{13}\text{C}\right]\text{glutamine} + \left[3, 4-^{13}\text{C}\right]\text{GABA} + \left[2, 3-^{13}\text{C}\right]\text{aspartate}\right)} \quad (7)$$

## Cycling Ratios from 2nd and 1st Turn of the TCA Cycle in Glutamate, Glutamine and GABA

The cycling ratios give information on how long the label stays in the TCA cycle before it is incorporated into glutamate, glutamine and other metabolites. Cycling ratios of label from [ $^{13}\text{C}$ ]glucose and [ $^{13}\text{C}$ ]acetate were calculated from rats injected with [ $1, 2-^{13}\text{C}$ ]glucose and those receiving [ $1, 2-^{13}\text{C}$ ]acetate and [ $1-^{13}\text{C}$ ]glucose, respectively. The cycling ratios for glutamate and glutamine from both [ $1, 2-^{13}\text{C}$ ]glucose and [ $1, 2-^{13}\text{C}$ ]acetate can be calculated using the same equation (Eq. 8). Cycling ratios cannot be calculated for GABA due to similar labelling patterns from [ $1-^{13}\text{C}$ ]glucose and [ $1, 2-^{13}\text{C}$ ]acetate in the 2nd turn of the TCA cycle.

The cycling ratio for label from glucose and acetate in glutamate and glutamine synthesis will be:

$$\left(2 \times \left[1, 2-^{13}\text{C}\right]\right)\text{glutamate}(\text{glutamine}) / \left[4, 5-^{13}\text{C}\right]\text{glutamate}(\text{glutamine}) \quad (8)$$

## Transfer Ratio from Astrocytes to Neurons

Given that most of the glutamate in the brain is located in the neuronal compartment [11] and acetate is metabolised only in astrocytes [5], substantial labelling of [ $4, 5-^{13}\text{C}$ ]glutamate from [ $1, 2-^{13}\text{C}$ ]acetate can only happen with the help of [ $4, 5-^{13}\text{C}$ ]glutamine that is transferred from the astrocytic to the neuronal compartment. Thus, a ratio between [ $4, 5-^{13}\text{C}$ ]glutamate and [ $4, 5-^{13}\text{C}$ ]glutamine would reflect the transfer from astrocytes to neurons. Based upon this assumption, the transfer of substrate from astrocytes to glutamatergic neurons can be estimated as:

$$\% \text{ enrichment } \left[4, 5-^{13}\text{C}\right]\text{glutamate} / \% \text{ enrichment } \left[4, 5-^{13}\text{C}\right]\text{glutamine} \quad (9)$$

Similarly, an estimate of the transfer of substrate from astrocytes to GABAergic neurons can be made as:

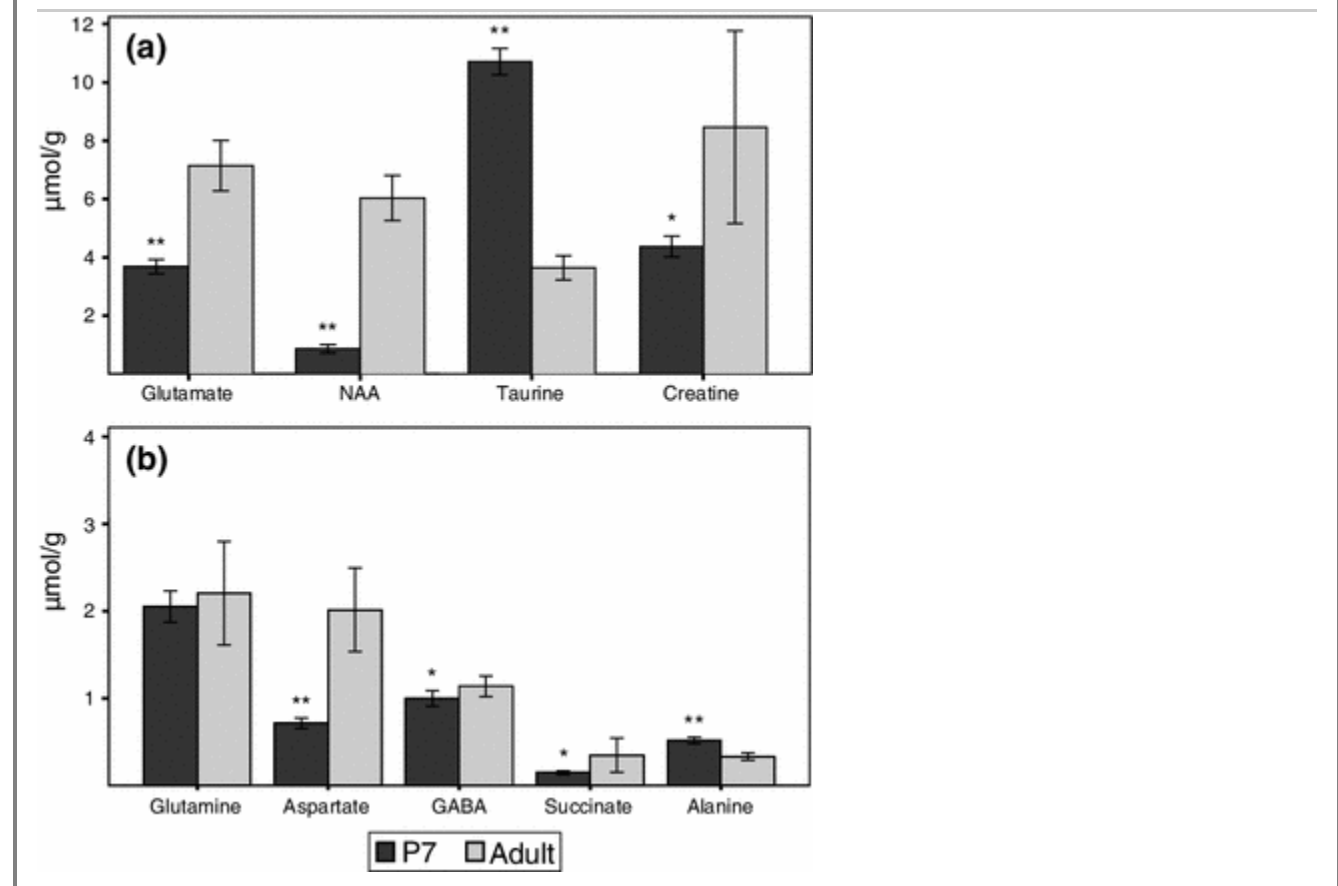
$$\% \text{ enrichment } \left[1, 2-^{13}\text{C}\right]\text{GABA} / \% \text{ enrichment } \left[4, 5-^{13}\text{C}\right]\text{glutamine} \quad (10)$$

## Statistics

Data are presented as mean  $\pm$  standard error of the mean (SEM) or means  $\pm$ 95 % confidence interval (only in Fig. 2). For two-group comparisons Levene's test for equal variances was performed, and the adequate Student's *t* test was used,  $p < 0.05$  was chosen as level of significance.

Fig. 2

Brain extracts from postnatal day 7 (*dark grey bars*) and adult (*light grey bars*) rats were analyzed by  $^1\text{H}$  NMRS ( $n = 10$  in each age group). For more details see "Materials and Methods". Results are presented as mean  $\pm$ 95 % CI. Unpaired Student's *t* test was used to compare P7 and adult rats. Asterisks indicate statistical difference from the same metabolite in adult rats.  $p$  values: \* $\leq 0.05$ , \*\* $\leq 0.001$



## Results

$^1\text{H}$  NMR spectra were used to quantify amounts of central metabolites, which are listed in Fig. 2. Taurine and alanine were the only metabolites which were higher in the neonatal compared to the adult brain. The neonatal brain had twofold lower levels of glutamate and several-fold lower levels of NAA and aspartate compared to the adult brain, while the levels of glutamine were similar, and those of GABA and succinate were only slightly smaller.

In order to obtain information about the time course for incorporation of  $^{13}\text{C}$  label into metabolites, rat pups were injected with  $[1-^{13}\text{C}]$ glucose plus  $[1,2-^{13}\text{C}]$ acetate and decapitated at different time points, as earlier described. The  $^{13}\text{C}$  enrichments in brain glucose and acetate did not change significantly with time (Table 1). Pyruvate, the end-point of glycolysis, can be reduced to lactate or transaminated to alanine. Thus, the  $^{13}\text{C}$  labelling of lactate and alanine reflects glycolytic activity.

% Enrichment in alanine and lactate was quantifiable from 30 min onwards (Table 1). The maximum %  $^{13}\text{C}$  enrichment in pyruvate and thereby lactate and alanine is 50 % of %  $^{13}\text{C}$  enrichment in glucose. However the % enrichment in these metabolites was much smaller, indicating pyruvate formation via PPP activity and contributions from branched chain amino acids. Figure 3 shows the amounts of  $^{13}\text{C}$  label in different isotopomers of glutamate, glutamine and GABA at the different time points. At 15 min after injection  $^{13}\text{C}$  label in most metabolites was detectable, but small. By 30 min, the amounts of the first turn metabolites [ $4\text{-}^{13}\text{C}$ ]glutamate, [ $4\text{-}^{13}\text{C}$ ]glutamine and [ $2\text{-}^{13}\text{C}$ ]GABA were close to the maximum (Fig. 3). Thus, we decided to use a 30 min incorporation time for the labelling experiment with [ $1,2\text{-}^{13}\text{C}$ ]glucose in the P7 rats as well as for the major comparisons with adult rats. Experiments with adult rats were carried out with a 15 min waiting time after injection as earlier described [29–31]. Typical  $^{13}\text{C}$  NMR spectra from P7 rats 30 min after injection of [ $1\text{-}^{13}\text{C}$ ]glucose and [ $1,2\text{-}^{13}\text{C}$ ]acetate (a) and after injection of [ $1,2\text{-}^{13}\text{C}$ ]glucose (b) are shown in Fig. 4.

Table 1

Total amounts of glucose, lactate, alanine (nmol/g), % excess enrichment and amounts of [ $1\text{-}^{13}\text{C}$ ]glucose, [ $3\text{-}^{13}\text{C}$ ]lactate, [ $3\text{-}^{13}\text{C}$ ]alanine and [ $1,2\text{-}^{13}\text{C}$ ]acetate (nmol/g) in brain extracts from P7 rats injected with [ $1\text{-}^{13}\text{C}$ ]glucose and [ $1,2\text{-}^{13}\text{C}$ ]acetate

	Labelling time (min)				
	5 (n = 4)	10 (n = 3)	15 (n = 3)	30 (n = 4)	45 (n = 4)
Glucose					
Total amount	1,883 ± 207	2,253 ± 323	1,599 ± 88	1,363 ± 77	1,687 ± 184
[ $1\text{-}^{13}\text{C}$ ]Glc	146 ± 65	196 ± 37	132 ± 21	119 ± 12	125 ± 28
$^{13}\text{C}$ enrichment (%)	23.5 ± 8.9	30.0 ± 6.7	27.4 ± 3.5	29.1 ± 1.7	24.2 ± 3.5
Lactate					
Total amount	1,758 ± 397	9,322 ± 119	9,622 ± 84	3,453 ± 372	3,134 ± 344
[ $3\text{-}^{13}\text{C}$ ]Lac	na	na	na	204 ± 30	153 ± 12
$^{13}\text{C}$ enrichment (%)	na	na	na	6.0 ± 0.7	5.0 ± 0.3
Alanine					
Total amount	485 ± 18	363 ± 92	294 ± 55	536 ± 20	493 ± 37
[ $3\text{-}^{13}\text{C}$ ]Ala	na	na	na	39 ± 4	33 ± 3

<sup>13</sup> C enrichment (%)	na	na	na	7.2 ± 0.5	6.7 ± 0.7
Acetate					
[1,2- <sup>13</sup> C]Ace	412 ± 168	433 ± 99	653 ± 48	452 ± 38	307 ± 169

Postnatal day 7 rat pups were injected with [1-<sup>13</sup>C]glucose plus [1,2-<sup>13</sup>C]acetate and decapitated after 5, 10, 15, 30 and 45 min. Total amounts and those of <sup>13</sup>C-labelled metabolites are given as nmol/g wet weight. Brain extracts were analysed using <sup>1</sup>H-NMRS (glucose, lactate, alanine) and <sup>13</sup>C NMRS (acetate). For more details see “Materials and Methods“. Results are presented as mean ± SEM

Ace, acetate; Ala, alanine; Glc, glucose; Lac, lactate; na, natural abundant <sup>13</sup>C only

Fig. 3

Rat pups were injected with [1-<sup>13</sup>C]glucose and [1,2-<sup>13</sup>C]acetate on postnatal day 7. The animals were decapitated at 5 (n = 4), 10 (n = 3), 15 (n = 3), 30 (n = 4) and 45 (n = 4) minutes after injection. Brain extracts were analysed using <sup>13</sup>C-NRMS. For more details see “Materials and Methods“. The graphs represent the amounts of label in the different isotopomeres of glutamate (a), glutamine (b) and GABA (c). The y-axis in B has been truncated between 50 and 100 nmol/g, also the step size is different before and after the truncation. Results are presented as mean ± SEM

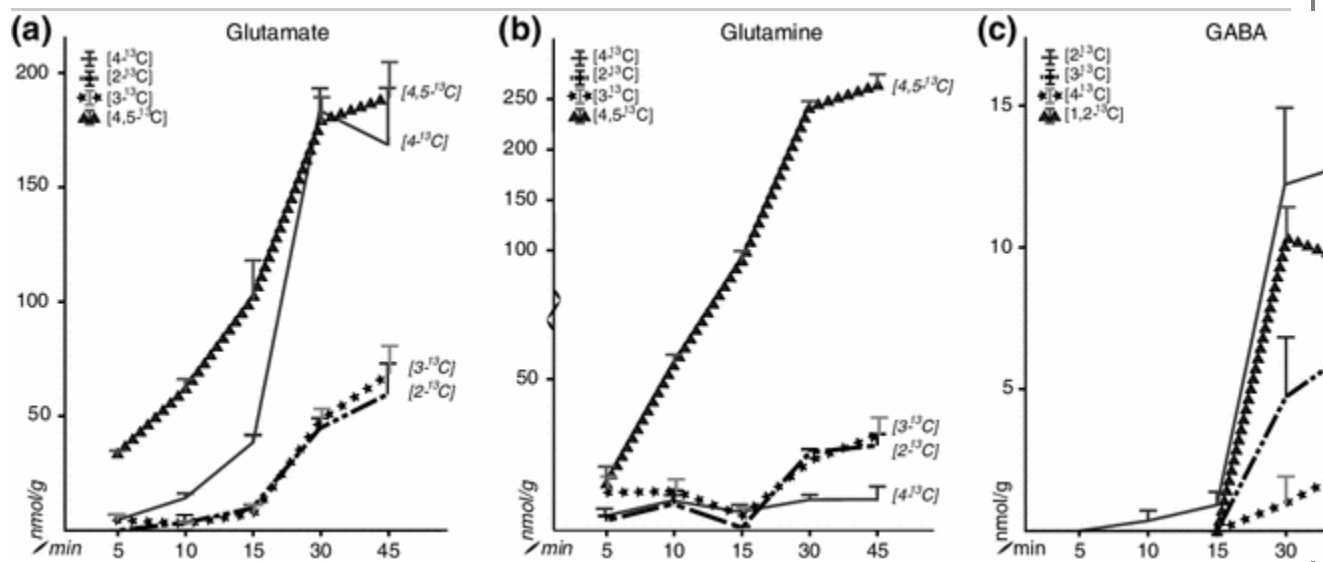
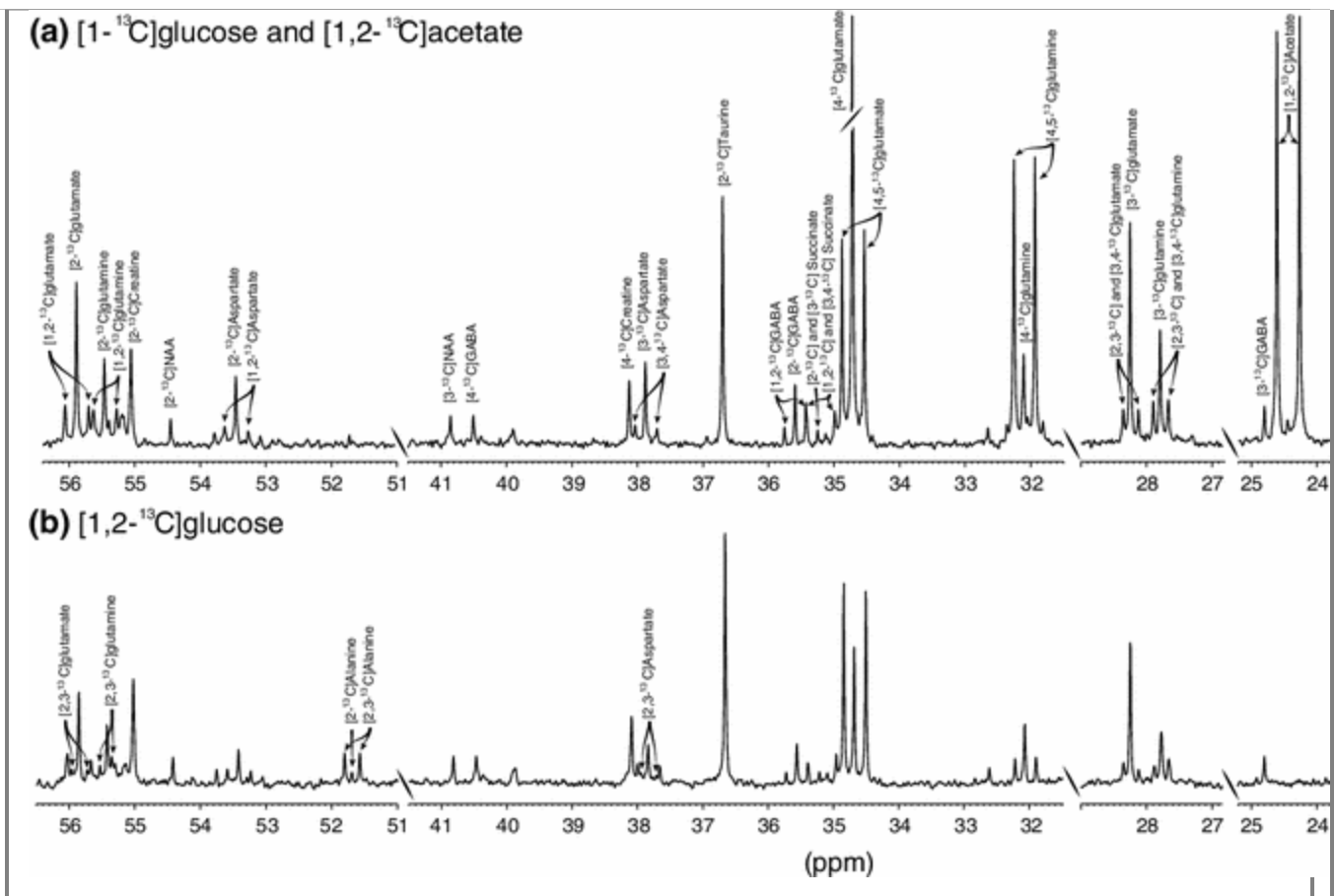


Fig. 4

<sup>13</sup>C MR spectra of the brain extracts from postnatal day 7 rats. The horizontal axis has been truncated in several places. **a** Spectrum resulting from metabolism of [1-<sup>13</sup>C]glucose and [1,2-<sup>13</sup>C]acetate. The peaks of [4-<sup>13</sup>C]glutamate and [3-<sup>13</sup>C]lactate have been truncated. **b** Spectrum resulting from metabolism of [1,2-<sup>13</sup>C]glucose. Most of the peaks are only marked in (a), but some additional doublets and singlets have been marked in (b). NAA, *n*-acetyl aspartate; ppm, parts per million



At all time-points, the amounts of  $^{13}\text{C}$  labelled isotopomers and the % enrichment from  $[1-^{13}\text{C}]$ glucose were lower for glutamate, glutamine and GABA in the neonatal versus adult brain (Table 2; Fig. 3). This difference was particularly pronounced for  $[4-^{13}\text{C}]$ glutamate. When comparing % enrichment of  $[4-^{13}\text{C}]$ glutamate after 15 min it can be calculated that  $[1-^{13}\text{C}]$ glucose metabolism was lower by a factor of six in the neonatal compared to adult brain (P7  $1.4 \pm 0.1\%$ ; adult  $7.7 \pm 0.6\%$ ,  $p \leq 0.001$ ). However, in  $[4-^{13}\text{C}]$ glutamine the % enrichment after 15 min was lower by a factor of eleven (P7  $0.4 \pm 0.1\%$ ; adult  $4.4 \pm 0.5\%$ ,  $p = 0.002$ ). Metabolism of  $[1,2-^{13}\text{C}]$ acetate 15 min after injection was 50 % lower in the neonatal compared to the adult brain, seen in the % enrichment of  $[4,5-^{13}\text{C}]$ glutamine (P7  $6.2 \pm 1.4\%$ ; adult  $14.4 \pm 1.4\%$ ,  $p = 0.009$ ) and similar to the adult in  $[4,5-^{13}\text{C}]$ glutamate (P7  $3.6 \pm 0.4\%$ ; adult  $3.1 \pm 0.7\%$ ,  $p = 0.31$ ). However, after 30 min the % enrichment in  $[4,5-^{13}\text{C}]$ glutamine in the neonatal brain was similar to that of the adult brain after 15 min (Table 2) and that of  $[4,5-^{13}\text{C}]$ glutamate was significantly higher. Amount and %  $^{13}\text{C}$  enrichment with  $[1,2-^{13}\text{C}]$ GABA was much smaller in neonates compared to in adults at all time points.

Table 2

Amounts of  $^{13}\text{C}$ -labelled isotopomers, % enrichment of and metabolic ratios for glutamate, glutamine and GABA derived from  $[1-^{13}\text{C}]$ glucose and  $[1,2-^{13}\text{C}]$ acetate

Amount (nmol/g)	Enrichment (%)
-----------------	----------------

	P7	Adult	<i>P</i> value	P7	Adult	<i>P</i> value
[2- <sup>13</sup> C]Glutamate	44.6 ± 4.5	207.4 ± 22.0	<0.001	1.0 ± 0.1	2.6 ± 0.3	0.003
[3- <sup>13</sup> C]Glutamate	48.0 ± 5.1	178.1 ± 18.6	0.001	1.1 ± 0.2	2.3 ± 0.3	0.009
[4- <sup>13</sup> C]Glutamate	183.7 ± 9.7	609.5 ± 51.2	<0.001	4.3 ± 0.4	7.7 ± 0.6	0.003
[4,5- <sup>13</sup> C]Glutamate	179.4 ± 9.9	244.4 ± 20.6	0.070	4.1 ± 0.3	3.1 ± 0.2	0.021
[2- <sup>13</sup> C]Glutamine	25.5 ± 2.6	81.3 ± 8.7	<0.001	1.1 ± 0.1	3.4 ± 0.5	0.008
[3- <sup>13</sup> C]Glutamine	23.0 ± 0.9	72.2 ± 6.6	<0.001	1.0 ± 0.1	3.1 ± 0.5	0.005
[4- <sup>13</sup> C]Glutamine	10.2 ± 1.5	103.6 ± 9.6	<0.001	0.5 ± 0.1	4.4 ± 0.5	<0.001
[4,5- <sup>13</sup> C]Glutamine	242.9 ± 5.1	348.2 ± 29.7	0.008	10.7 ± 0.7	14.4 ± 1.4	0.121
[2- <sup>13</sup> C]GABA	12.2 ± 2.7	64.9 ± 6.0	<0.001	1.2 ± 0.3	5.4 ± 0.6	0.001
[3- <sup>13</sup> C]GABA	4.7 ± 2.1	25.9 ± 3.3	0.002	0.5 ± 0.2	2.2 ± 0.3	0.008
[4- <sup>13</sup> C]GABA	1.0 ± 1.0	33.3 ± 3.9	<0.001	0.1 ± 0.1	2.8 ± 0.4	0.001
[1,2- <sup>13</sup> C]GABA	10.3 ± 1.1	29.2 ± 3.4	<0.001	1.0 ± 0.1	2.4 ± 0.3	0.016
<i>Acetate versus glucose utilisation</i>						
Glutamate (Eq. 1)	0.98 ± 0.05	0.40 ± 0.02	<0.001			
Glutamine (Eq. 1)	25.82 ± 4.43	3.47 ± 0.29	0.015			
GABA (Eq. 2)	0.92 ± 0.13	0.47 ± 0.06	0.003			
<i>Acetate cycling ratio</i>						
Glutamate (Eq. 8)	0.54 ± 0.01	0.57 ± 0.02	0.297			
Glutamine (Eq. 8)	0.40 ± 0.02	0.43 ± 0.02	0.580			
<i>Transfer between astrocytes and neurons</i>						
Ast-Glu Neu (Eq. 9)	0.37 ± 0.02	0.22 ± 0.02	<0.001			
Ast-GABA Neu (Eq. 10)	0.09 ± 0.01	0.17 ± 0.05	0.014			

Postnatal day 7 rat pups (n = 4) and adult rats (n = 10) were injected with [1-<sup>13</sup>C]glucose and [1,2-<sup>13</sup>C]acetate and decapitated after 30 and 15 min respectively. Brain extracts were analysed using <sup>13</sup>C- and <sup>1</sup>H-NMRS. For calculation of equations (Eq.) and % enrichment see “Materials and Methods”. Results are presented as mean ± SEM. Unpaired *Student's t* test was used to compare P7 and adult rats

Ast, astrocyte; Eq., equation; GABA, GABAergic; Glu, glutamatergic; Neu, neuron

The neonatal brain utilised significantly more acetate relative to glucose compared to that of adults, particularly for glutamine synthesis, but also the synthesis of the neurotransmitters glutamate and GABA (Table 2). There was no detectable 2nd turn labelling from [1,2-<sup>13</sup>C]acetate metabolism until 30 min after injection. However, after 30 min the cycling ratio of label from [1,2-<sup>13</sup>C]acetate in relation to glutamate and glutamine was similar in the P7 rats compared to adults (Eq. 8). Due to very high acetate utilisation and peak overlap in the C3-positions a reliable cycling ratio for glucose could not be calculated from the experiment with [1-<sup>13</sup>C]glucose and [1,2-<sup>13</sup>C]acetate. It could, however, be calculated from the experiment using [1,2-<sup>13</sup>C]glucose (Table 3 and 4), which gave a cycling ratio for glutamate of  $0.27 \pm 0.02$ , while there was no detectable 2nd turn labelling from PDH-related GM in glutamine except in one sample.

Table 3

Amounts of <sup>13</sup>C-labelled isotopomers and % enrichment of key metabolites derived from [1,2-<sup>13</sup>C]glucose

	Amounts (nmol/g)	Enrichment (%)
[2,3- <sup>13</sup> C]Lactate	148.6 ± 26.7	9.78 ± 0.62
[3- <sup>13</sup> C]Lactate	17.1 ± 3.9	1.11 ± 0.13
[2,3- <sup>13</sup> C]Alanine	27.7 ± 2.8	5.09 ± 0.76
[3- <sup>13</sup> C]Alanine	2.7 ± 0.7	0.47 ± 0.12
[1,2- <sup>13</sup> C]Glutamate	17.8 ± 3.2	0.46 ± 0.07
[2,3- <sup>13</sup> C]Glutamate	10.9 ± 1.8	0.30 ± 0.06
[4,5- <sup>13</sup> C]Glutamate	127.5 ± 13.1	3.39 ± 0.39
[2- <sup>13</sup> C]Glutamate	3.2 ± 2.0	0.09 ± 0.06
[3- <sup>13</sup> C]Glutamate	11.0 ± 2.4	0.30 ± 0.09

[4- <sup>13</sup> C]Glutamate	11.7 ± 2.0	0.31 ± 0.06
[5- <sup>13</sup> C]Glutamate	na	na
[1,2- <sup>13</sup> C]Glutamine	nq	nq
[2,3- <sup>13</sup> C]Glutamine	14.1 ± 1.9	0.6 ± 0.1
[4,5- <sup>13</sup> C]Glutamine	13.8 ± 2.0	0.6 ± 0.1
[2- <sup>13</sup> C]Glutamine	3.6 ± 1.1	0.16 ± 0.04
[3- <sup>13</sup> C]Glutamine	2.8 ± 1.0	0.13 ± 0.04
[4- <sup>13</sup> C]Glutamine	na	na
[5- <sup>13</sup> C]Glutamine	nq	nq
[1,2- <sup>13</sup> C]GABA	4.6 ± 0.1	0.48 ± 0.03
[3,4- <sup>13</sup> C]GABA	nq	nq
[2- <sup>13</sup> C]GABA	0.7 ± 0.6	0.08 ± 0.06
[1,2- <sup>13</sup> C]Aspartate	10.2 ± 1.0	1.29 ± 0.13
[2,3- <sup>13</sup> C]Aspartate	3.4 ± 1.2	0.42 ± 0.15
[3,4- <sup>13</sup> C]Aspartate	12.6 ± 0.9	1.62 ± 0.18

Postnatal day 7 rat pups (n = 4) were injected with [1,2-<sup>13</sup>C]glucose and decapitated after 30 min. Brain extracts were analysed using <sup>13</sup>C- and <sup>1</sup>H-NMRS. For calculation of % enrichment and more details see “Materials and Methods”. Results are presented as mean ± SEM

na, no detectable label except natural abundance; nq, not quantifiable

Table 4

Metabolic ratios for metabolites derived from [1,2-<sup>13</sup>C]glucose

PPP/GM (%)	
Lactate (Eq. 3)	14.40 ± 0.84
Alanine (Eq. 3)	12.98 ± 3.62



Glutamate (Eq. 4)	11.86 ± 0.98
PC/PDH	
Glutamate (Eq. 5)	0.09 ± 0.001
Glutamine (Eq. 5)	1.09 ± 0.22
GABA (Eq. 6)	nc
Cycling ratio	
Glucose	
Glutamate (Eq. 8)	0.27 ± 0.02
Glutamine (Eq. 8)	nc

Postnatal day 7 rat pups (n = 4) were injected with [1,2-<sup>13</sup>C]glucose and decapitated after 30 min. Brain extracts were analysed using <sup>13</sup>C- and <sup>1</sup>H-NMRS. For calculation of equations (Eq.) see “Materials and Methods”. Results are presented as mean ± SEM

Eq., equation; GM, glucose metabolism; nc, not possible to calculate since one or more of the necessary peaks for the calculation were not quantifiable; PDH, Pyruvate dehydrogenase; PPP, Pentose-phosphate pathway

The metabolism of glucose via PPP was studied using [1,2-<sup>13</sup>C]glucose as injection (Table 3). PPP related labelling was evidenced by the appearance of [3-<sup>13</sup>C]lactate, [3-<sup>13</sup>C]alanine, [4-<sup>13</sup>C]glutamate [2-<sup>13</sup>C]glutamine and [2-<sup>13</sup>C]GABA. These isotopomers (except for [2-<sup>13</sup>C]glutamine) could in theory also be obtained via pyruvate recycling [27, 28] which would in addition lead to formation of equal amounts of [5-<sup>13</sup>C]glutamate. Analysis of the presence of [5-<sup>13</sup>C]glutamate was used to evaluate the possibility of labelling via pyruvate recycling. [5-<sup>13</sup>C]glutamate was not labelled above natural abundance (Table 3; Fig. 4). Thus, it was concluded that correction for pyruvate recycling was not necessary and that the PPP accounted for around 10 % of GM in relation to lactate, alanine and glutamate (Table 4). In [4-<sup>13</sup>C]glutamine there was no detectable labelling from [1,2-<sup>13</sup>C]glucose above natural abundance (Table 3; Fig. 4). The labelling of this position is dependent on PPP activity followed by PDH activity. However, there was more labelling in [2-<sup>13</sup>C]glutamine (Table 3) compared to [3-<sup>13</sup>C]glutamine, a difference that can only come from PPP activity followed by PC activity. The C2 and C3 positions can also be labelled from cycling, but given the undetectable cycling ratio in glutamine, it is likely that most of the labelling in both [3-<sup>13</sup>C]- and [2-<sup>13</sup>C]glutamine is from PPP followed by PC (with/without backflux).

Analysis of data from experiments with [1,2-<sup>13</sup>C]glucose makes it also possible to study the pyruvate carboxylation via PC and compare it to pyruvate dehydrogenation via PDH (Table 3). There were similar amounts of [4,5-<sup>13</sup>C]glutamine (from PDH) and [2,3-<sup>13</sup>C]glutamine (from PC)

seen in the PC/PDH ratio that was close to 1, while glutamate clearly contained more label via PDH compared to PC (Table 4). In the adult brain the PC/PDH ratio for glutamine has been found to be 0.35 (calculated from [32] based on isotopomer labelling reported in their Table 1 combined with Eq. 5 described in the “Methods” section above). However in the adult brain, a confounding factor for the PC/PDH ratio in glutamine is the transfer to astrocytes of glutamate labelled via PDH in the neuronal compartment. This will give rise to overestimation of PDH in glutamine synthesis since this glutamate will be converted to glutamine in the astrocytic compartment. In the adult brain 40 % of glutamine in astrocytes arises from glutamate labelled via neuronal PDH [33]. Therefore, by subtracting 40 % of PDH in the calculation of PC/PDH in adults from Kunnecke et al. [32] the ratio with only astrocytic PDH in glutamine in adults would be  $0.35/(1-0.4) \approx 0.6$ . However, in the neonatal brain the low percent enrichment in  $[4-^{13}\text{C}]$ glutamine from  $[1-^{13}\text{C}]$ glucose indicates that the transfer of glutamate from the neuronal to the astrocytic compartment is very low. Therefore we can assume that the detectable PDH labelling in glutamine arises from astrocytic PDH. Using Eq. 7, we estimated the contribution of PC to pyruvate metabolism to be  $14.5 \pm 1.1$  %.

The transfer of glutamate, glutamine and GABA between the cellular compartments was different in the neonatal brain compared to adults (Table 2). The transfer of glutamate from glutamatergic neurons to astrocytes was much lower than in the adult brain as evidenced by the low ratio of % enrichment of  $[4-^{13}\text{C}]$ glutamine over  $[4-^{13}\text{C}]$ glutamate from  $[1-^{13}\text{C}]$ glucose ( $0.11 \pm 0.02$  in the neonatal brain vs.  $0.56 \pm 0.04$  in the adult brain,  $p < 0.001$ ). In contrast, the transfer of glutamine from astrocytes to glutamatergic neurons was almost doubled in the neonatal compared to adult brain as evidenced by the high labelling with  $[4,5-^{13}\text{C}]$ glutamate when compared to labelling with  $[4,5-^{13}\text{C}]$ glutamine (Eq. 9; Table 2). By also considering the transfer ratio from astrocytes to glutamatergic neurons at 15 min (Eq. 9 =  $0.58 \pm 0.03$ ), it was verified that the relatively higher transfer of substrate was not just due to longer labelling time. However, the transfer from astrocytes to GABAergic neurons was lower than in the adult brain at both 30 and 15 min (Eq. 10).

## Discussion

### Glucose Utilisation

It is well established that glucose is the almost exclusive fuel in the adult, but not the developing brain [1]. The number of glucose transporters in the BBB, GLUT-1, is low in the neonatal brain and rises sharply after the second postnatal week in the period of neuronal maturation and brain growth spurt [3, 34]. However, transport over the BBB does not appear to be a limiting factor since the amount and % enrichment of glucose in the brain on postnatal day 7 detected in the present study were similar to levels published for the adult brain [27, 35]. After entry, a low glucose utilisation rate in P6 rat brain has been reported [36]. In agreement with this lower glycolytic activity was shown directly in the present study by the lower levels of  $^{13}\text{C}$  incorporation from  $[1-^{13}\text{C}]$ glucose at all time-points in lactate and alanine compared to data published for the adult brain [27, 35]. Furthermore, it has been suggested that it is the glucose transporter GLUT-3 on neurons that is the rate-limiting factor for cerebral glucose utilisation and not transporters in the BBB [37].

TCA cycle enzyme levels are low in the neonatal compared to adult brain [8] corresponding well with the six-times lower metabolism of glucose derived metabolites via the TCA cycle observed in this study evidenced in glutamate labelling. This reduction is also supported by the smaller amount of the TCA cycle intermediate succinate and the lower cycling ratios of glucose-derived isotopomers of glutamate ( $0.27 \pm 0.02$ ) and glutamine (too small to calculate) compared to those in

adults ( $0.46 \pm 0.0$  and  $0.77 \pm 0.1$ , respectively) [38]. Furthermore, our observations are in agreement with a previous report of lower TCA cycle turnover of label from  $[1-^{13}\text{C}]$ glucose in the postnatal period [7].

### Acetate Utilisation

In the adult, transport of  $[1,2-^{13}\text{C}]$ acetate over the BBB (via MCT-1) must be slower than metabolism of acetate since acetate is present in serum but not detectable in the brain as reported by Melo et al. [39], and in the present study. However, in the neonatal brain, transport over the BBB exceeds metabolism as evidenced by the presence of  $[1,2-^{13}\text{C}]$ acetate in the brain on P7 shown in this study (Fig. 4; Table 1). This may be due to the high expression of MCT-1 in the BBB of the neonate, which decreases after weaning [3]. 15 min after injection of  $[1,2-^{13}\text{C}]$ acetate, its metabolism in the neonatal brain was lower than in adults by a factor of two. However with longer labelling time (30 min), % enrichment in  $[4,5-^{13}\text{C}]$ glutamine was similar in the neonatal and adult brain and the TCA cycling of label was similar. Acetate metabolism has earlier been reported to be higher in P10 versus P30 rat brain [7]. The label distribution in glutamine, glutamate and GABA from  $[1,2-^{13}\text{C}]$ acetate obtained in the present study demonstrates that also in P7 rats, acetate is predominantly or exclusively metabolised in astrocytes. Furthermore, in the P7 animals relatively more  $[1,2-^{13}\text{C}]$ acetate was used for both glutamine and glutamate synthesis than  $[1-^{13}\text{C}]$ glucose compared to the adult brain (acetate/glucose utilisation ratios in Table 2), affirming that GM via pyruvate dehydrogenase was much lower on P7 compared to adults.

### Pyruvate Carboxylation (Anaplerosis)

As mentioned in “Methods”, the de novo synthesis of neurotransmitter amino acids is only possible via pyruvate carboxylase in astrocytes [9, 10]. Whereas the glutamine content was similar, that of glutamate, aspartate and NAA was much lower in neonatal than in adult brain, as has earlier been reported [18]. Thus, to build up pools of neurotransmitter from neonatal to adult age, there is a necessity for a close collaboration between astrocytes and neurons. PC activity has been reported to increase from birth to adult age by 15-fold [8]. Using  $[1,2-^{13}\text{C}]$ glucose it was possible to establish that approximately 50 % of glucose in astrocytes was metabolised via pyruvate carboxylation in neonatal rats since the PC/PDH ratio in glutamine was close to 1. Since the PC/PDH ratio in glutamine in adults is 0.6 (see “Results“ for details) this indicates that the pyruvate derived from the small amount of glucose entering the astrocytic compartment is to a larger extent used by PC than PDH in the neonatal compared to adult brain. The relative distribution between PC and whole brain PDH activity can be calculated to be 14.5 % by analysis of labelling patterns in glutamate, glutamine, aspartate and GABA. The equivalent value in adult brain is approximately 10 % [40].

### The Glutamate-Glutamine Cycle

In adult brain the glutamate-glutamine cycle is essential for efficient glutamatergic neurotransmission:  $[4-^{13}\text{C}]$ glutamate released from neurons is mostly taken up into astrocytes and is converted into  $[4-^{13}\text{C}]$ glutamine and sent back to the neurons for conversion to glutamate. This is different in the neonatal brain as evidenced by the low ( $0.5 \pm 0.1$ ) % enrichment with  $[4-^{13}\text{C}]$ glutamine, indicating negligible transport of glutamate from neurons to astrocytes. This may be due to a number of factors: little glutamate release by the neurons which are building up their glutamate pool; increased reuptake by neurons; or reduced uptake by the astrocytes. Transfer from astrocytes to neurons can be followed by analysing the % enrichment of glutamate and glutamine

with [4,5-<sup>13</sup>C]glutamate and [4,5-<sup>13</sup>C]glutamine respectively (Eq. 9). It is evident from the transfer ratio (Table 2) that transfer of glutamine from astrocytes to neurons was relatively higher in the neonatal compared to the adult brain. This indicates that only the part of the glutamate-glutamine cycle transferring glutamine from astrocytes to neurons is operating in the neonatal brain.

## GABA

Consistent with earlier reports GABA content was only slightly smaller in the neonatal compared to the adult brain [7, 18]. This is in agreement with the finding that on P7 the density of GABAergic neurons is similar to that in the adult brain [41]. The PC/PDH ratio was not quantifiable in GABA, which is an indication that the main de novo synthesis of GABA has already happened before this developmental stage. While GABA content was only slightly lower, incorporation and turnover of <sup>13</sup>C-label was much lower in the neonatal compared to adult brain. Also, the transfer of glutamine from astrocytes to GABAergic neurons was lower than in the adult brain. This indicates that GABAergic neurons have the ability to take up GABA from the synapse early in brain development [42, 43] and therefore are less dependent on anaplerosis by astrocytes.

## PPP

The PPP/GM ratio in the neonatal brain (11–14 %) was much higher than that reported for adults (2–5 %) [21–23]. In fact it was at levels comparable to those reported after stress such as traumatic brain injury in adult human and rodent brain [24, 25]. Activity of the PPP was evident in neurons due to the presence of [4-<sup>13</sup>C]glutamate. <sup>13</sup>C label was also detectable in [2-<sup>13</sup>C]glutamine which is synthesized via PPP and thereafter PC (Table 3), confirming earlier reports that the PPP is present in both neurons and astrocytes [44]. There are several reasons why the neonatal brain needs to prioritise glucose for the PPP; such as production of NADPH for GSH reduction, lipid and nucleotide synthesis. We did not find evidence for pyruvate recycling on postnatal day 7, which is in agreement with an earlier report of undetectable pyruvate recycling until postnatal day 14 [45].

## Conclusion

Neuronal-astrocytic interactions in the neonatal brain were very different from those in adult brain. The negligible transfer of glutamate from neurons to astrocytes combined with the high transfer of glutamine from astrocytes to neurons indicates that only a part of the glutamate-glutamine cycle works in early brain development, thus operating as a delivery system of substrate from astrocytes to neurons. This makes <sup>13</sup>C labelled glucose combined with isotopomer analysis particularly suited for mapping of neuronal metabolism in early brain development. Overall GM was five times lower in neonatal brain. However, the relative amount of glucose that was metabolised via PPP and anaplerosis (PC) was higher than in adults. The combination of reduced uptake of glutamate in astrocytes and a high PPP/GM ratio may have implications for the neonatal brain and its ability for protection against excitotoxicity and oxidative stress. Future studies should investigate the significance of these findings in models of disease.

## Acknowledgments

This work was supported by a grant from the Liaison Committee between St. Olav University Hospital and Norwegian University of Science and Technology (NTNU; to TSM) and from the Medical Faculty at NTNU (EB). The NMRS was performed at the MR Core Facility at NTNU. The

technical assistance of Lars Evje is gratefully acknowledged.

## References

- [1] Cremer JE (1982) Substrate utilization and brain development. *J Cereb Blood Flow Metab* 2(4):394–407. doi:10.1038/jcbfm.1982.43
- [2] McKenna MC, Tildon JT, Stevenson JH, Hopkins IB (1994) Energy metabolism in cortical synaptic terminals from weanling and mature rat brain: evidence for multiple compartments of tricarboxylic acid cycle activity. *Dev Neurosci* 16(5–6):291–300
- [3] Vannucci SJ, Simpson IA (2003) Developmental switch in brain nutrient transporter expression in the rat. *Am J Physiol Endocrinol Metab* 285(5):E1127–E1134. doi:10.1152/ajpendo.00187.2003
- [4] Waniewski RA, Martin DL (1998) Preferential utilization of acetate by astrocytes is attributable to transport. *J Neurosci* 18(14):5225–5233
- [5] Sonnewald U, Westergaard N, Schousboe A, Svendsen JS, Unsgard G, Petersen SB (1993) Direct demonstration by [<sup>13</sup>C]NMR spectroscopy that glutamine from astrocytes is a precursor for GABA synthesis in neurons. *Neurochem Int* 22(1):19–29
- [6] Qu H, Haberg A, Haraldseth O, Unsgard G, Sonnewald U (2000) (<sup>13</sup>C) MR spectroscopy study of lactate as substrate for rat brain. *Dev Neurosci* 22(5–6):429–436. doi:17472
- [7] Chowdhury GMI, Patel AB, Mason GF, Rothman DL, Behar KL (2007) Glutamatergic and GABAergic neurotransmitter cycling and energy metabolism in rat cerebral cortex during postnatal development. *J Cereb Blood Flow Metab* 27(12):1895–1907
- [8] Wilbur DO, Patel MS (1974) Development of mitochondrial pyruvate metabolism in rat brain. *J Neurochem* 22(5):709–715
- [9] Patel MS (1974) The relative significance of CO<sub>2</sub>-fixing enzymes in the metabolism of rat brain. *J Neurochem* 22(5):717–724
- [10] Yu AC, Drejer J, Hertz L, Schousboe A (1983) Pyruvate carboxylase activity in primary cultures of astrocytes and neurons. *J Neurochem* 41(5):1484–1487
- [11] Storm-Mathisen J, Leknes AK, Bore AT, Vaaland JL, Edminson P, Haug FM, Ottersen OP (1983) First visualization of glutamate and GABA in neurones by immunocytochemistry. *Nature* 301(5900):517–520
- [12] Norenberg MD, Martinez-Hernandez A (1979) Fine structural localization of glutamine synthetase in astrocytes of rat brain. *Brain Res* 161(2):303–310

- [13] Danbolt NC (2001) Glutamate uptake. *Prog Neurobiol* 65(1):1–105
- [14] Aghajanian GK, Bloom FE (1967) The formation of synaptic junctions in developing rat brain: a quantitative electron microscopic study. *Brain Res* 6(4):716–727
- [15] Boulland J-L, Rafiki A, Levy LM, Storm-Mathisen J, Chaudhry FA (2003) Highly differential expression of SN1, a bidirectional glutamine transporter, in astroglia and endothelium in the developing rat brain. *Glia* 41(3):260–275. doi:10.1002/glia.10188
- [16] Weiss MD, Derazi S, Rossignol C, Varoqui H, Erickson JD, Kilberg MS, Anderson KJ (2003) Ontogeny of the neutral amino acid transporter SAT1/ATA1 in rat brain. *Dev Brain Res* 143(2):151–159. doi:10.1016/s0165-3806(03)00107-x
- [17] Furuta A, Rothstein JD, Martin LJ (1997) Glutamate transporter protein subtypes are expressed differentially during rat CNS development. *J Neurosci* 17(21):8363–8375
- [18] Tkac I, Rao R, Georgieff MK, Gruetter R (2003) Developmental and regional changes in the neurochemical profile of the rat brain determined by in vivo 1H NMR spectroscopy. *Magn Reson Med* 50(1):24–32. doi:10.1002/mrm.10497
- [19] Yager JY, Ashwal S (2009) Animal models of perinatal hypoxic-ischemic brain damage. *Pediatr Neurol* 40(3):156–167
- [20] Baquer NZ, Hothersall JS, McLean P, Greenbaum AL (1977) Aspects of carbohydrate metabolism in developing brain. *Dev Med Child Neurol* 19(1):81–104
- [21] Hostetler KY, Landau BR (1967) Estimation of the pentose cycle contribution to glucose metabolism in tissue in vivo. *Biochemistry* 6(10):2961–2964
- [22] Ben-Yoseph O, Boxer P, Ross B (1996) Noninvasive assessment of the relative roles of cerebral antioxidant enzymes by quantitation of pentose phosphate pathway activity. *Neurochem Res* 21(9):1005–1012. doi:10.1007/bf02532410
- [23] Gaitonde MK, Evison E, Evans GM (1983) The rate of utilization of glucose via hexosemonophosphate shunt in brain. *J Neurochem* 41(5):1253–1260
- [24] Dusick JR, Glenn TC, Lee WN, Vespa PM, Kelly DF, Lee SM, Hovda DA, Martin NA (2007) Increased pentose phosphate pathway flux after clinical traumatic brain injury: a [1,2-13C2]glucose labeling study in humans. *J Cereb Blood Flow Metab* 27(9):1593–1602. doi:10.1038/sj.jcbfm.9600458
- [25] Bartnik BL, Sutton RL, Fukushima M, Harris NG, Hovda DA, Lee SM (2005) Upregulation of pentose phosphate pathway and preservation of tricarboxylic acid cycle flux after experimental brain injury. *J Neurotrauma*

22(10):1052–1065. doi:10.1089/neu.2005.22.1052

- [26] Brekke EM, Walls AB, Schousboe A, Waagepetersen HS, Sonnewald U (2012) Quantitative importance of the pentose phosphate pathway determined by incorporation of  $^{13}\text{C}$  from [2- $^{13}\text{C}$ ]- and [3- $^{13}\text{C}$ ]glucose into TCA cycle intermediates and neurotransmitter amino acids in functionally intact neurons. *J Cereb Blood Flow Metab* 32(9):1788–1799. doi:10.1038/jcbfm.2012.85
- [27] Melø TM, Nehlig A, Sonnewald U (2006) Neuronal-glia interactions in rats fed a ketogenic diet. *Neurochem Int* 48(6–7):498–507
- [28] McKenna MC, Dienel GA, Sonnewald U, Waagepetersen HS, Schousboe A (2012) Energy metabolism of the brain. In: *Basic neurochemistry*, 8th edn. Elsevier, London, pp 224–253
- [29] Alvestad S, Hammer J, Qu H, Haberg A, Ottersen OP, Sonnewald U (2011) Reduced astrocytic contribution to the turnover of glutamate, glutamine, and GABA characterizes the latent phase in the kainate model of temporal lobe epilepsy. *J Cereb Blood Flow Metab* 31(8):1675–1686. doi:10.1038/jcbfm.2011.36
- [30] Hassel B, Sonnewald U, Fonnum F (1995) Glial-neuronal interactions as studied by cerebral metabolism of [2- $^{13}\text{C}$ ]acetate and [1- $^{13}\text{C}$ ]glucose: an ex vivo  $^{13}\text{C}$  NMR spectroscopic study. *J Neurochem* 64(6):2773–2782
- [31] Kanamatsu T, Tsukada Y (1994) Measurement of amino acid metabolism derived from [1- $^{13}\text{C}$ ]glucose in the rat brain using  $^{13}\text{C}$  magnetic resonance spectroscopy. *Neurochem Res* 19(5):603–612
- [32] Kunnecke B, Cerdan S, Seelig J (1993) Cerebral metabolism of [1,2- $^{13}\text{C}_2$ ]glucose and [U- $^{13}\text{C}_4$ ]3-hydroxybutyrate in rat brain as detected by  $^{13}\text{C}$  NMR spectroscopy. *NMR Biomed* 6(4):264–277
- [33] Hassel B, Bachelard H, Jones P, Fonnum F, Sonnewald U (1997) Trafficking of amino acids between neurons and glia in vivo. Effects of inhibition of glial metabolism by fluoroacetate. *J Cereb Blood Flow Metab* 17(11):1230–1238. doi:10.1097/00004647-199711000-00012
- [34] Vannucci SJ (1994) Developmental expression of GLUT1 and GLUT3 glucose transporters in rat brain. *J Neurochem* 62(1):240–246. doi:10.1046/j.1471-4159.1994.62010240.x
- [35] Eyjolfsson EM, Nilsen LH, Kondziella D, Brenner E, Haberg A, Sonnewald U (2011) Altered  $^{13}\text{C}$  glucose metabolism in the cortico-striato-thalamo-cortical loop in the MK-801 rat model of schizophrenia. *J Cereb Blood Flow Metab* 31(3):976–985. doi:10.1038/jcbfm.2010.193
- [36] Dombrowski GJ Jr, Swiatek KR, Chao KL (1989) Lactate, 3-hydroxybutyrate, and glucose as substrates for the early postnatal rat brain. *Neurochem Res* 14(7):667–675

- [37] Vannucci SJ, Seaman LB, Brucklacher RM, Vannucci RC (1994) Glucose transport in developing rat brain: glucose transporter proteins, rate constants and cerebral glucose utilization. *Mol Cell Biochem* 140(2):177–184. doi:10.1007/bf00926756
- [38] Kondziella D, Brenner E, Eyjolfsson EM, Markinhuhta KR, Carlsson ML, Sonnewald U (2006) Glial-neuronal interactions are impaired in the schizophrenia model of repeated MK801 exposure. *Neuropsychopharmacology* 31(9):1880–1887. doi:10.1038/sj.npp.1300993
- [39] Melo TM, Nehlig A, Sonnewald U (2005) Metabolism is normal in astrocytes in chronically epileptic rats: a  $(13)\text{C}$  NMR study of neuronal-glia interactions in a model of temporal lobe epilepsy. *J Cereb Blood Flow Metab* 25(10):1254–1264. doi:10.1038/sj.jcbfm.9600128
- [40] Hertz L (2011) Astrocytic energy metabolism and glutamate formation —relevance for  $13\text{C}$ -NMR spectroscopy and importance of cytosolic/mitochondrial trafficking. *Magn Reson Imaging* 29(10):1319–1329. doi:10.1016/j.mri.2011.04.013
- [41] Micheva KD, Beaulieu C (1995) Postnatal development of GABA neurons in the rat somatosensory barrel cortex: a quantitative study. *Eur J Neurosci* 7(3):419–430
- [42] Vitellaro-Zuccarello L, Calvaresi N, Biasi S (2003) Expression of GABA transporters, GAT-1 and GAT-3, in the cerebral cortex and thalamus of the rat during postnatal development. *Cell Tissue Res* 313(3):245–257. doi:10.1007/s00441-003-0746-9
- [43] Sipilä S, Huttu K, Voipio J, Kaila K (2004) GABA uptake via GABA transporter-1 modulates GABAergic transmission in the immature hippocampus. *J Neurosci* 24(26):5877–5880. doi:10.1523/jneurosci.1287-04.2004
- [44] Ben-Yoseph O, Boxer PA, Ross BD (1996) Assessment of the role of the glutathione and pentose phosphate pathways in the protection of primary cerebrocortical cultures from oxidative stress. *J Neurochem* 66(6):2329–2337. doi:10.1046/j.1471-4159.1996.66062329.x
- [45] Cruz F, Scott SR, Barroso I, Santisteban P, Cerdan S (1998) Ontogeny and cellular localization of the pyruvate recycling system in rat brain. *J Neurochem* 70(6):2613–2619



